UCRL-20372

A STUDY OF SLIP BAND GROWTH IN PRESTRAINED COPPER

Thomas H. Kosel
(M. S. Thesis)

December 1970

AEC Contract No. W-7405-eng-48

LAWRENCE RADIATION LABORATORY
UNIVERSITY of CALIFORNIA BERKELEY

UCRL-20372

DISCLAIMER

PAGES i to ii

WERE INTENTIONALLY

LEFT BLANK

CONTENTS

THIS PAGE

WAS INTENTIONALLY

LEFT BLANK

A STUDY OF SLIP BAND GROWTH IN PRESTRAINED COPPER

Thomas H. Kosel

Inorganic Materials Research Division, Lawrence Radiation Laboratory, Department of Materials Science and Engineering, College of Engineering, University of California, Berkeley, California

ABSTRACT

The formation of heavy slip bands in prestrained copper crystals was studied by transmission electron microscopy. Heavily damaged regions parallel to the primary slip plane were observed. These were found to correlate well in dimensions and distribution with slip bands observed in a previous surface investigation[1] of crystals of the same geometry. The damaged regions consisted principally of dense carpets of dislocations lying on the primary glide plane. The observations are discussed in terms of a model which explains the formation of heavy slip bands.

INTRODUCTION

It is known that in pure FCC metal crystals which have been radiation hardened or quench hardened there exists an initial low hardening region of the stress-strain curve which is associated with the appearance of sharp slip markings on the surface.[1,2,3,4] It has been observed by transmission electron microscopy (TEM) that during the low hardening transient the damage introduced by quenching or irradiating the crystals is "swept out" along certain glide layers by slip on the primary system.[4] This creates in effect a softened path in the crystal which may be followed by more slip along the same or nearby glide layers, creating a heavy slip band with a large step height.

It is also known that heavy prestraining of FCC crystals by any of several means (including shock loading,[1] twisting,[3] and tension in easy glide[2] or polyslip orientation[1] causes subsequent straining in a single slip orientation to exhibit an initial region of low hardening and coarse slip markings on the surface. Thus, Murty and Washburn[1] were led to suggest that the mechanism responsible for the coarse slip markings and initial low hardening rate in prestrained crystals was similar to that thought to be responsible for these effects in quench hardened and irradiation hardened crystals. They noted that the tangled "walls" of the dislocation cell structure introduced by prestraining (consisting of "cells" of nearly perfect crystal separated by tangled "walls" of dislocations) commonly exhibit only very small net lattice rotations across them. This indicates that within the tangles there are nearly equal numbers of dislocations having the positive and negative

sign of each Burgers vector present, so that the net Burgers vector taken over a large Burgers circuit is small. Therefore the cell wall tangles must be metastable in the sense that rearrangements within them which allow dislocation segments with equal but opposite Burgers vectors to come together can in theory annihilate most of the tangles. It was suggested that local rearrangements of this type could be caused by slip on a new slip system, causing a soft path through which large numbers of primary dislocations could pass to form a heavy slip band.

A satisfactory theory to account for the low hardening rate of these prestrained crystals should explain the fact that the gradual change in the character of slip from fine slip lines to coarse slip bands with increasing prestrain is accompanied by a gradual increase in the extent and decrease in the slope of the low hardening region of the stress strain curve (Fig. 1). This gradual change in both the character of slip and the stress-strain curve strongly suggests that Stage I of an as-grown crystal should be explained in the same way that the initial low strain hardening rate of prestrained crystals is explained. In both as-grown and prestrained crystals slip is distributed unevenly along the gage length of the crystal prior to the transition to a higher strain hardening rate. This transition occurs when the whole gage length has been filled with slip lines or bands.(1)

Once the softened path in the prestrain dislocation structure has been produced, slip on a slip line can proceed until hardening mechanisms due to primary slip causes the softened path to regain the same "hardness" as the rest of the dislocation structure. At higher stress levels (and higher prestrains) more hardening should be necessary to stop individual

slip lines, and so more dislocations should move in each slip line. That the dislocation distribution produced by slip on one slip plane is stable with respect to further slip on the same slip plane but not to slip on other slip planes has been demonstrated by Basinski and Jackson.[2] Coupled with the greater number of slip lines (due to their clustering closer together) this means that more dislocations will move in a heavily prestrained crystal before the gage length is covered with slip bands so that Stage I will be longer. The increasing tendency to form a Lüders band with increasing prestrain indicates that new slip bands form in parts of the crystal which are more nearly characteristic of the prestrain. If each new slip band forms under exactly the same conditions as previous bands, the strain hardening rate must be zero. Therefore the increasing tendency towards Lüders band formation should be accompanied by a decreasing strain hardening rate in Stage I , as observed.

The present TEM work was undertaken to discover whether evidence of local annihilation of cell wall tangels could be discovered in the dislocation structure of the crystal after the second deformation. The work was carried out on crystals given a heavy prestrain. Since heavily prestrained crystals generally show one or more Lüders bands spreading over the surface TEM foils were taken from areas of the crystals having slip markings characteristic of the Lüders band, the area near the front of the Lüders band and the more or less undeformed area into which the Lüders band was propagating. Foils of different orientations were examined.

EXPERIMENTAL

A large single crystal (3.5x1x15 cm) was grown in an induction furnace using a split graphite mold and ASARC 99.999% pure copper. After electron beam welding OFHC copper grips to the ends the crystal was prestrained along [111] to a resolved shear stress of 2.5 kg/mm^2. The crystal orientation is illustrated in Fig. 2 . Smaller crystals (1x1 cm cross section) of a single slip orientation were then removed from the large crystal by spark machining. These had as their primary slip plane the (111) plane which was perpendicular to the prestrain tensile axis (Fig. 2). The ends of the small crystals were cut off perpendicular to the crystal axis by spark machining so that the crystals could be deformed in compression. The spark cut faces of these crystals were then removed to a depth of about 1 mm with an acid polishing wheel; the other faces were also polished to obtain a smooth surface for slip line observation. The ends of the crystals were then lightly sanded using a jig designed to make them very flat and parallel. The crystals were then deformed at room temperature in compression using an Instron testing machine at a strain rate of $5x10^{-5}$ sec^{-1}.

After compression to a point in Stage I of the stress-strain curve, the crystals were sectioned on various crystallographic planes by acid sawing. The slices obtained (about 1 mm thick) were then thinned to 0.002 in. to 0.003 in. with the acid polishing wheel. Discs 3 mm in diameter were chemically removed from these thin sections via a photo resist method. The copper was dipped in Kodak Photo Resist (thinned 50%) and allowed to dry. It was then placed between two sheets of film which were prepared with clear circles on a black background (with the film taped so the circles were in register) and exposed about a minute to sunlight. After

one minute developing in Kodak Photo Resist developer and dying , the photo resist was allowed to dry for several hours. Imperfections in the resist were touched up with lacquer before dissolving away the copper surrounding the discs in a two molar solution of $FeCl_3$. The photo resist was dissolved away in acetone; usually a residual film remained which was carefully removed with tweezers. Dipping in an acid mixture (two parts HNO_3, one part HPO_4 and one part HAc) helped to loosen the film. The resutling discs were electropolished in a Fischione jet electropolishing machine using a solution of one part HNO_3 and two parts methanol. A voltage of 5-10 volts with 10-20 mA current at -40°C gave consistently good foils. Foils were examined in an Hitachi HU125 electron microscope at 125 kV, and in a 650 kV Hitachi microscope operated at 500 kV to prevent electron radiation damage.(5)

Small misorientations (about 1/2 deg rotation) were observed, and these were studied by taking selected area diffraction patterns using an aperature of 20 microns in diameter, which selected an area in the image of about 1/2 micron in diameter. Shifting of the Kikuchi lines relative to the spots in the diffraction pattern gave a measure of the magnitude and direction of the lattice rotations. These determinations were carried out at 500 kV to minimize the uncertainty in the area selected which is introduced by spherical abberation.(6)

The primary slip system was defined as having the Burgers vector $b_p = a/2[10\bar{1}]$ and the primary slip plane (111). Several foil orientations were examined: $(1\bar{2}1)$, $(11\bar{2})$, and $(10\bar{1})$ foils (perpendicular to the primary slip plane); and (hkl) foils (at 45° to the slip plane). Most observations were made on $(1\bar{2}1)$ foils; large composite micrographs were made to study the long range variations in dislocation structure and to

select "representative" areas without bias. The orientations of the primary plane, and the cross-slip, conjugate, and critical planes are illustrated for (hkl), $(1\bar{2}1)$, and $(10\bar{1})$ foils in Fig. 3.

RESULTS

The dislocation distribution introduced by straining in tension along [111] has been studied by Price and Washburn[7]. It consists of a dislocation cell structure in which the cells are essentially isotropic; no significant tendency for dislocations or tangles to lie on any specific plane exists in such crystals. A representative view of this cell structure taken at 500 kV using a $(1\bar{2}1)$ foil from the prestrained crystal, is shown in Fig. 4 . The cell size is roughly 3 to 4 microns.

$(1\bar{2}1)$ FOILS

In the $(1\bar{2}1)$ foils the primary slip plane lies perpendicular to the plane of the foil and b_p, the primary Burgers vector, lies in the plane of the foil. The cross-slip plane along the same line ($[10\bar{1}]$) as does the primary plane if the plane of the foil is accurately $(1\bar{2}1)$; the conjugate and critical planes have traces at 68° to the $[10\bar{1}]$ direction (Fig. 3a).

$(1\bar{2}1)$ foils taken after the second deformation had a very different appearance than foils taken after the prestrain. Very dense carpets of dislocations lying on the primary slip plane were observed. These carpets occurred both singly and (very frequently) in pairs separated by 1/2 to 1 micron and running parallel over distances of about 10 microns (Fig. 5). Fairly large misorientations between one side and the other of single carpets were common. The region enclosed between paired carpets of dislocations was almost always tilted with respect to the surrounding crystal by one half to one degree. These misorientations produced changes of contrast in the micrographs and were undoubtedly associated with local internal stresses. If a given pair of carpets was surrounded by crystal which was oriented near the Bragg condition (i.e. strongly transmitting)

and enclosed an area which was not (i.e. weakly transmitting) then the relative contrast could usually be reversed by tilting the foil slightly in the microscope (Fig. 6). Selected area diffraction studies were carried out at 500 kV to determine the magnitude and axis of these lattice rotations. It was found that the axis and magnitude of the rotations varied from one carpet (or pair of carpets) to the next, and along the length of a given carpet or pair of carpets. The magnitude of the rotations varied between zero and one degree being usually about one half degree. These rotations are considered in the discussion.

The dislocations in the carpets were mostly not of the primary Burgers vector. In fact, the appearance of carpets did not change appreciably when the operating reflection was changed from one which left primary dislocations in contrast (e.g. $g = 1\bar{1}3$ or $g = 20\bar{2}$; $g \cdot b_p = 0$) to the (111) reflection, for which all dislocations having Burgers vectors which lie in the primary slip plane (i.e. a/2 $[10\bar{1}]$, a/2 $[1\bar{1}0]$, and a/2 $[01\bar{1}]$ are out of contrast (Figs.7,8).Thus the carpets were mainly composed of dislocations having the Burgers vectors which lie out of the primary slip plane: ± a/2 [101], ± a/2 [110], and ± a/2 [011]. Micrographs taken with the primary dislocations in contrast (Figs.7a,8a,9) showed primary dislocations occurring in the cell wall tangles near the carpets, and between the carpets. They are distinguished from dislocations lying in other planes by the fact that they must be straight lines lying on the trace of the primary slip plane unless they are very heavily jogged.

Foils which were taken from the Luders band section of a crystal showed more of the paired and unpaired carpets than foils taken from parts of the crystal having only a few slip bands on the surface. Foils

showing essentially no slip bands on the surface were observed to have only a few carpets and paired carpets of dislocations. The dislocation network in the crystal near the carpets had a very similar appearance to that observed in the prestrained crystal prior to the second deformation.

The average spacing between paired carpets (1/2 micron) agreed well with Murty's result for the slip band width in such crystals. Any determination of the length of an individual slip band is necessarily somewhat subjective. First of all, what we see in the micrographs is the distribution of dislocations which remains after straining; therefore, what we identify as a slip band is the dislocation "damage" which is left behind after a large amount of primary slip has occurred. It is quite conceivable that in places along the length of a slip band only a small amount of visible damage is left behind, due to local conditions. Secondly, as noted by Murty, with increasing prestrain there is an increasing tendency for slip bands to nucleate near the end of previously formed bands. In our micrographs the paired carpets of dislocations usually extended 10 to 20 microns, but evidence of slip (single carpets) on the same group of glide layers frequently extended for as much as 100 microns.

Because our observations were of the dislocation damage which is left after passage of the slip bands it was not possible to provide any definite evidence either for or against the idea of local cell wall annihilation by primary slip. This is because the annihilation of part of a cell wall tangle is usually followed by the formation of new tangles due to the passage of large numbers of primary dislocations. Once in a while an area such as Fig. 7 was observed in thin foils; this

can be interpreted as a case of local annihilation. It should be noted here that if cell wall annihilation does not occur over a large part of a cell wall the likelihood of observing the broken tangle could be quite small.

(11$\bar{2}$) FOILS

A few (11$\bar{2}$) foils were examined to determine whether interchanging the orientation of the cross-slip, conjugate and critical planes would produce any significant changes in the appearance of the dislocation networks. No such differences were found.

(10$\bar{1}$) FOILS

In (10$\bar{1}$) foils the plane of the foil is perpendicular to the primary Burgers vector and to the primary glide plane. In these foils primary dislocations are always out of contrast since $g \cdot b_p = 0$ for all possible reflections. The cross-slip plane is also seen edge-on in (10$\bar{1}$) foils, and it makes an angle of 70° to the primary slip plane. The conjugate and critical planes make an angle of 35° to the plane of the foil and have a common trace which lies at 55° to both the primary and cross-slip planes (Fig.3b).

The carpets and paired carpets of dislocations observed in the (1$\bar{2}$1) foils were also observed in (10$\bar{1}$) foils. In some areas there were also large numbers of individual dislocations and dislocation tangles lying on the trace of the cross-slip plane or very close to it. Carpets of dislocations in such areas sometimes "jumped" from one glide layer to another one a fraction of a micron away at the intersection with dense tangles on the cross-slip plane (Fig. 10). In these areas the more or less isotropic rounded cells characteristic of the prestrain were absent

(Fig.10). These areas were interpreted as having undergone very heavy slip in the second deformation, and occurred in the Luders band of the crystals.

In less heavily deformed parts of $(10\bar{1})$ foils the dislocation distribution was very similar in appearance to that in $(1\bar{2}1)$ foils (Fig. 11a, 12a). The length of "slip bands" was roughly half what was observed in $(1\bar{2}1)$ sections.

Very significant changes in the appearance of the carpets were observed when the operating reflection was changed from g = 111 to g = $1\bar{1}1$ (Fig.11,12).In such cases the density of dislocations in contrast was found to decrease markedly. Thus, the great majority of dislocations present in the carpets had the Burgers vectors ± a/2 [110] and ± a/2 [011]. Primary dislocations were of course out of contrast for both reflections.

(hkl) FOILS

In (hkl) foils both the primary slip plane and the primary Burgers vector make an angle of 45° to the plane of the foil (Fig. 3c). (hkl) foils were taken both within 100 μ of the surface of the crystal and from the interior of the crystal to see whether there was any noticeable difference between the dislocation arrangement in the surface and the bulk. No significant difference was found. Slip bands were somewhat difficult to identify since the primary plane was not viewed edge-on, but it was concluded that they were essentially the same in both cases. An example is shown in Fig. 13 .

DISCUSSION

The carpets and paired carpets of dislocations observed after the second deformation are assumed to be the damage left behind by the passage of heavy slip bands. This assumption is supported by the observation that the dimensions of the slip bands agree well with the dimensions of the damaged regions observed in the dislocation networks. In addition the appearance of the surface slip bands (Fig. 14) suggests that there may be a correlation between the heaviest individual slip lines within a slip band and the individual carpets of dislocations seen in the interior. The question of the mechanism for forming these slip bands remains.

It is commonly observed in FCC crystals oriented for single slip that although the strain on secondary slip systems is very small compared to strain on the primary slip system, the density of secondary dislocations becomes approximately equal to the density of primary dislocations early in Stage II of the stress-strain curve.[8,9,10,11] This observation is accounted for by assuming that the secondary slip distance is small; many dislocations moving small distances produce only small strains. The reason that dislocations on secondary slip systems move only short distances even when the resolved shear stress on their slip system has passed the stress at which Stage I normally begins must be that the secondary dislocations meet tangles caused by slip on the primary system. Secondary systems are thus "hardened" by primary slip, and the lack of extensive slip on secondary systems is attributed to latent hardening of these systems. Hirsch and Mitchell[12,13] consider that secondary dislocations are generated under the combined influence of the applied stress and local

internal stresses attending piled up groups of primary dislocations. This combined stress acts on sources of secondary dislocations. In the present case of prestrained crystals, carpets of dislocations are observed which lie on the primary slip plane and which are commonly composed of dislocations belonging to secondary slip systems. This suggests that the dislocations in the carpets are produced by the action of secondary dislocation sources under the influence of internal stresses caused by a nearby accumulation of primary dislocations. It is important to note here that the stress field of a group of primary dislocations can act to push dislocations of a secondary slip system away, or to pull negative dislocations of the same system into the primary dislocations. In the latter case the secondary dislocations may form attractive junctions with the primary dislocations and make a tangle of dislocations on the primary slip plane which can act to impede further primary slip. Once one of these carpets is started on a glide layer (or group of nearby glide layers) its growth will be almost certain, since primary dislocations which come up against such a barrier which is long on their glide plane will be stopped and can in turn help to operate nearby sources of secondary dislocations. The growth of such a carpet depends on the availability of suitable secondary dislocation sources. The absence of such sources could cause a gap in the carpet such as that observed in Fig.5,7. Extensive cross-slip may occur by thermal activation or intersection mechanisms [14] in such regions, but will probably not allow all primary dislocations to circumvent the obstacle.

The existence of the carpets can thus be fairly well understood by considering them to be the tangles which are formed in the wake of a

heavy slip line (I will refer to heavy slip on a few closely spaced glide layers as a slip line; several slip lines make up a slip band). However, this provides no insight as to the way that large numbers of primary dislocations are able to find or clear a path through the dense dislocation networks in order to allow extensive slip on the same few glide layers before a carpet is formed.

Since the slip bands are observed to extend over distances large compared to the dimensions of the cells, it is clear that either the accumulation of primary dislocations against the cell walls is able to operate primary sources on the other side of the tangles, or that their accumulation is able to cause rearrangements and partial annihilation within some parts of the cell wall tangles. The first alternative seems unlikely because it requires that sources of primary dislocations be quite common. This is not likely because slip tends to cluster more and more with increasing prestrain, indicating that slip line sources are less and less common. The fact that slip bands are usually nucleated near the stress concentration at an edge of the crystal also suggests a lack of good slip line sources. Whatever the mechanism of slip band formation may be, slip band sources must become less common with increasing prestrain because they increasingly form preferentially only at points of stress concentration near the ends of previously formed slip bands. This leads to the formation of Lüders bands in heavily prestrained crystals. The idea of cell wall annihilation is indirectly supported by the observation that the rounded, isotropic cells of the prestrain are replaced by a new dislocation distribution in heavily deformed parts of the Lüders band (Fig. 10). The cell wall tangles are

clearly not stable in the presence of large amounts of slip on the new slip plane.

Murty's description of the way surface slip band markings "run a relay race across the crystal" suggests that local stress concentrations near the ends of slip bands can act to nucleate new slip bands in much the same way that martensite plates are thought to nucleate new plates. The misorientations associated with the carpets of dislocations indicate the presence of local stress concentrations which should assist the operation of new primary dislocation sources. In addition, new primary sources may be produced in these areas by cross-slip or by recombination of dislocations moving to accomodate stress concentrations on secondary slip systems. The partial recombination within tangles which produced a soft path for widening of a slip line must extend for some distance above and below the slip line, and this should at some points make nucleation of a new slip line near the first easier. The extent of this affected zone should decrease with increasing prestrain, causing tighter clustering of slip lines within slip bands.

The general picture of the formation of a sharp slip line is then that a source, operating within a region of stress concentration, clears a path through some parts of the dense tangles of dislocations, allowing passage of many primary dislocations. At particularly impenetrable tangles, primary dislocations pile up and the resulting stress concentration acts on secondary dislocation sources to create a dense carpet of dislocations on the active glide layer, and also makes more likely the activation of nearby primary dislocation sources which can nucleate a new slip line. The appearance of two or more carpets of

dislocations near one another must then be due to the passage of two or more sharp slip lines near one another.

Two carpets will form near each other when two active slip lines encounter the same impenetrable tangle, or when they are stopped by near by obstacles so that carpets grow back along the slip planes until they overlap.

A slip line is a cross section through an area of active slip on a slip plane; therefore the damaged areas (carpets) we observe are not necessarily continuous. A view looking down on the primary glide plane might at some time look like that shown schematically in Fig. 15. At some places the slip path may loop back on itself, as at A and B. In some areas the conditions may exist for the formation of carpets (in the shaded area), while in other parts of the slipped area impenetrable obstacles may not have been met (in the unshaded area). Places may also exist where slip cannot proceed but where conditions do not exist for the formation of a carpet (e.g. along CD). The slip line can grow in some directions with increasing stress until it meets the conditions necessary to form a carpet; the formation of a carpet along the whole perimeter should stop further growth. This is consistent with Murty's observation that some slip lines continue to grow during a large increment in average strain.

The type of secondary dislocation sources which exist in different parts of the crsytal must also be different. This would explain the observation that the misorientations associated with carpets vary from place to place, since the carpets would be made up of different proportions of different kinds of dislocations at different places.

Although ± a/2 [110] and ± a/2 [011] dislocations were predominant in many carpets, there usually were other dislocations present, and the proportions of ± a/2 [110] and ± a/2 [011] dislocations can also vary.

When two carpets overlap one another, if one is formed before the other, the second one must be formed in the stress field associated with the first. This stress field can be somewhat relieved by forming a carpet nearby which contains an excess of dislocations with the opposite sign of the Burgers vector present in the first carpet (the Burgers vector referred to is the composite of excess Burgers vectors in the carpet). Thus the stress field of the first carpet favors the formation of a carpet nearby which minimizes the strain energy of the crystal. In addition, the primary dislocations which are responsible for the formation of the two carpets may well be of opposite signs. This would explain the complementary rotations which are observed in the case of paired carpets (Fig. 5,6).

Dislocations with the Burgers vectors ± a/2 [110] and ± a/2 [011] were observed to make up a very large part of the tangled carpets of dislocations. Judging from the appearance of these dislocations, unless they are extremely jogged they cannot lie on the cross-slip plane because they do not lie on the trace of $(1\bar{1}1)$ in the $(10\bar{1})$ foils (Fig. 10, 11, 12). Thus they must lie on the conjugate and critical planes, and they are mainly of edge character. An excess of the two Burgers vectors + a/2 [110] and + a/2 [011] would result in a lattice rotation about the $[3\bar{2}3]$ direction because edge dislocations produce rotations about the direction of the dislocation lines ($[1\bar{1}2]$ and $[2\bar{1}1]$ respectively). An excess of the two Burgers vectors + a/2 [110] and

- a/2 [011], or of the pair - a/2 [110] and + a/2 [110], would result in a lattice rotation about the $[10\bar{1}]$ direction. If the g vector used for a micrograph lies along the axis of rotation of the local misorientations observed, then the misorientation should cause no contrast effect. Micrographs taken with $g = 10\bar{1}$ in $(1\bar{2}1)$ foils showed contrast effects due to the misorientations, so $[10\bar{1}]$ can not be the axis of rotation. Since high order reflections give very poor micrographs, no micrographs were taken with $g = 6\bar{4}6$ in $(10\bar{1})$ foils.

The selected area diffraction experiments carried out on $(1\bar{2}1)$ foils did not yield a definite axis of rotation for the misorientations associated with carpets. In different places along carpets the axis was found to be different. Shifts of Kikuchi lines along the $[10\bar{1}]$ direction and along the [111] direction relative to the spot pattern, were observed in different cases. Shifts in directions representing a combination of these two directions were also observed. It is not possible to tell whether the axis of such small lattice rotations lies in the plane of the foil or not. If it does not, then both the spot pattern and the Kikuchi pattern must rotate about the transmitted beam; in other words the whole diffraction pattern must be somewhat rotated about the column of the microscope. Since this rotation is at most a fraction of a degree, it cannot be observed within experimental error. Because of this and the observed variation of the axis of rotation from place to place, it was not possible to determine the axis of rotation or the type of dislocations responsible for it.

The flow stress for the slip band forming process we have considered is controlled by the difficulty of moving dislocations through the

"softened" area of the slip line. Rather than one or a few dislocations creating this soft path it seems reasonable to consider that the annihilation is accomplished by groups of dislocations piling up against one barrier after another. In this case the stress for forming the slip line and for continuous slip in the line will be more or less the same. If this were not the case one would expect a serrated stress-strain curve in which slip bands were nucleated at a high stress and propagated at a lower stress. Slip lines would also be constrained to always form completely in a small strain interval, contrary to Murty's observations.

The rate of strain hardening of a crystal depends essentially on how much slip can occur at a given stress before slip band sites are exhausted. In Stage I many slip bands form and the stress remains nearly constant until the whole gage length is uniformly covered with slip bands. The strain hardening rate of Stage II of prestrained crystals is less than that observed in as-grown crystals. As Murty pointed out, the appearance of slip bands on crystals is nearly independent of the strain, the strain history, and the strain hardening rate. Crystals having quite different strain hardening rates (due to prestrain) form very similar slip bands at the same stress level. Carpets of dislocations lying parallel to the primary glide plane are a commonly observed feature of the dislocation networks of FCC single crsytals strained into late Stage II.[15,16,17] Slip lines formed during Stage II of as-grown crystals at the same stress as those formed in Stage I of a prestrained crystal may therefore form by the same mechanism. In this case the last increment of slip in an as-grown crystal (in Stage II), before reaching the stress at which Stage II of

the prestrained crystal begins, takes place by the formation of heavy slip bands similar to those which cover the gage length of the prestrained crystal in Stage I.

CONCLUSIONS

1. Single slip deformation of copper crystals prestrained in a polyslip orientation produces dense carpets and pairs of carpets of dislocations.
2. These carpets lie on the primary slip plane and have dimensions and spacings which correspond to the dimensions and spacings of slip bands observed on the crystal surface.
3. The appearance of the slipped areas does not change appreciably between the bulk of the crystal and 100μ from the crystal surface.
4. The formation of these slip bands can be explained by a model which assumes some local annihilations of cell wall tangles and the formation of dense carpets by interactions of primary and secondary dislocations.
5. The carpets are often made up almost entirely of dislocations having the Burgers vectors a/2[110] and a/2[011], and lying on the critical and conjugate planes, respectively.
6. The carpets usually contain excess dislocations of one sign of some Burgers vectors. This causes the occurrence of misorientations across the carpets which must be associated with local internal stresses.
7. The axis of these misorientations varies from place to place, indicating that the proportion of dislocations of different Burgers vectors also varies.

ACKNOWLEDGMENT

The author wishes to express his gratitude for the continuing support and encouragement of Prof. J. Washburn. He is also grateful for the assistance of Mr. Doug Kreitz in working out the photo-resist process, and of Mr. J. Patenaude for his assistance in the machine shop. This work was done under the auspices of the U. S. Atomic Energy Commission.

REFERENCES

1. J. Washburn and G. Murty, Can. J. Phys. 45, 523 (1967).
2. P. J. Jackson and Z. S. Basinski, Can. J. Phys. 45, 707 (1967).
3. J. V. Sharp and M. J. Makin, Can. J. Phys. 45, 519 (1967).
4. J. L. Strudel and J. Washburn, Phil. Mag. 9, 491 (1964).
5. M. J. Makin, Phil. Mag. 18, 637 (1968).
6. P. B. Hirsch, Electron Microscopy of Thin Crystals, Butterworths 1965, p. 18.
7. J. Washburn and W. L. Price, J. Aust. Inst. 8, 1 (1963).
8. F. R. N. Nabarro, Z. S. Basinski, and D. B. Holt, Adv. in Physics 13, 193 (1964).
9. T. E. Mitchell, Prog. Appl. Mat. Res. 6, 117 (1964).
10. D. Kuhlman-Wilsdorf, Bull. Amer. Phys. Soc. 12, 548 (1967).
11. T. E. Mitchell and P. R. Thornton, Phil. Mag. 10, 315 (1964).
12. P. B. Hirsch and T. E. Mitchell, Can. J. Phys. 45, 663 (1967).
13. Z. S. Basinski and T. E. Mitchell, Phil. Mag. 13, 103 (1966).
14. J. Washburn, Appl. Phys. Lett. 7, 183 (1965).
15. U. Essmann, Phys. Stat. Sol. 12, 707 (1965).
16. J. W. Steeds, Proc. Roy. Soc. Ser. A. 292, 343 (1966).
17. D. M. Moon and W. H. Robinson, Can. J. Phys. 45, 1017 (1967).

FIGURE CAPTIONS

Except where indicated electron micrographs were taken at 500 kV

Fig. 1. A family of stress-strain curves of copper crystals prestrained to different stresses. (Courtesy of G. Murty[1])

Fig. 2. Geometry of the crystals; the manner in which small crystals were removed from the large crystal is indicated. (Courtesy of G. Murty[1])

Fig. 3. Orientations of the primary, cross-slip, conjugate and critical planes for a) $(1\bar{2}1)$ foils

b) $(10\bar{1})$ foils

c) $(hk\ell)$ foils

Fig. 4. $(1\bar{2}1)$ Section of the large crystal after the prestrain deformation. The trace of the (111) plane, inactive during the prestrain, is shown.

Fig. 5. (121) Foil taken after the second deformation. g = 111. A fairly large area of the foil is shown.

Fig. 6. Shows the change of contrast in an area between a pair of carpets; the foil was tilted slightly between micrographs. $(1\bar{2}1)$ foil, 125 kV.

Fig. 7. $(1\bar{2}1)$ foil. In a), g = 111, $g \cdot b_p = 0$; in b), g = $\bar{1}13$, $g \cdot b_p \neq 0$; 125 kV.

Fig. 8. $(1\bar{2}1)$ foil. In a), g = 111, $g \cdot b_p = 0$; in b), g = $\bar{1}13$, $g \cdot b_p \neq 0$.

Fig. 9. $(1\bar{2}1)$ Foil; g = $\bar{1}13$, $g \cdot b_p \neq 0$.

Fig. 10. $(10\bar{1})$ Foil, from a very heavily deformed part of the Lüders band. Traces of the primary and cross-slip planes are indicated.

Fig. 11. $(10\bar{1})$ Foil. In a), g = 111; in b), g = $1\bar{1}1$.

Fig. 12. $(10\bar{1})$ Foil. In a), g = 111; in b), g = $1\bar{1}1$.

Fig. 13. (hkℓ) Foil taken after the second deformation. g = 020; $g \cdot b_p \neq 0$.

Fig. 14. Appearance of surface slip bands on the (hkℓ) face of a crystal prestrained to 2.54 kg/mm^2. (Courtesy of G. Murty[1])

Fig. 15. Schematic representation of the possible appearance of a slip line looking down on the primary glide plane. The shaded region indicates a carpet of dislocations.

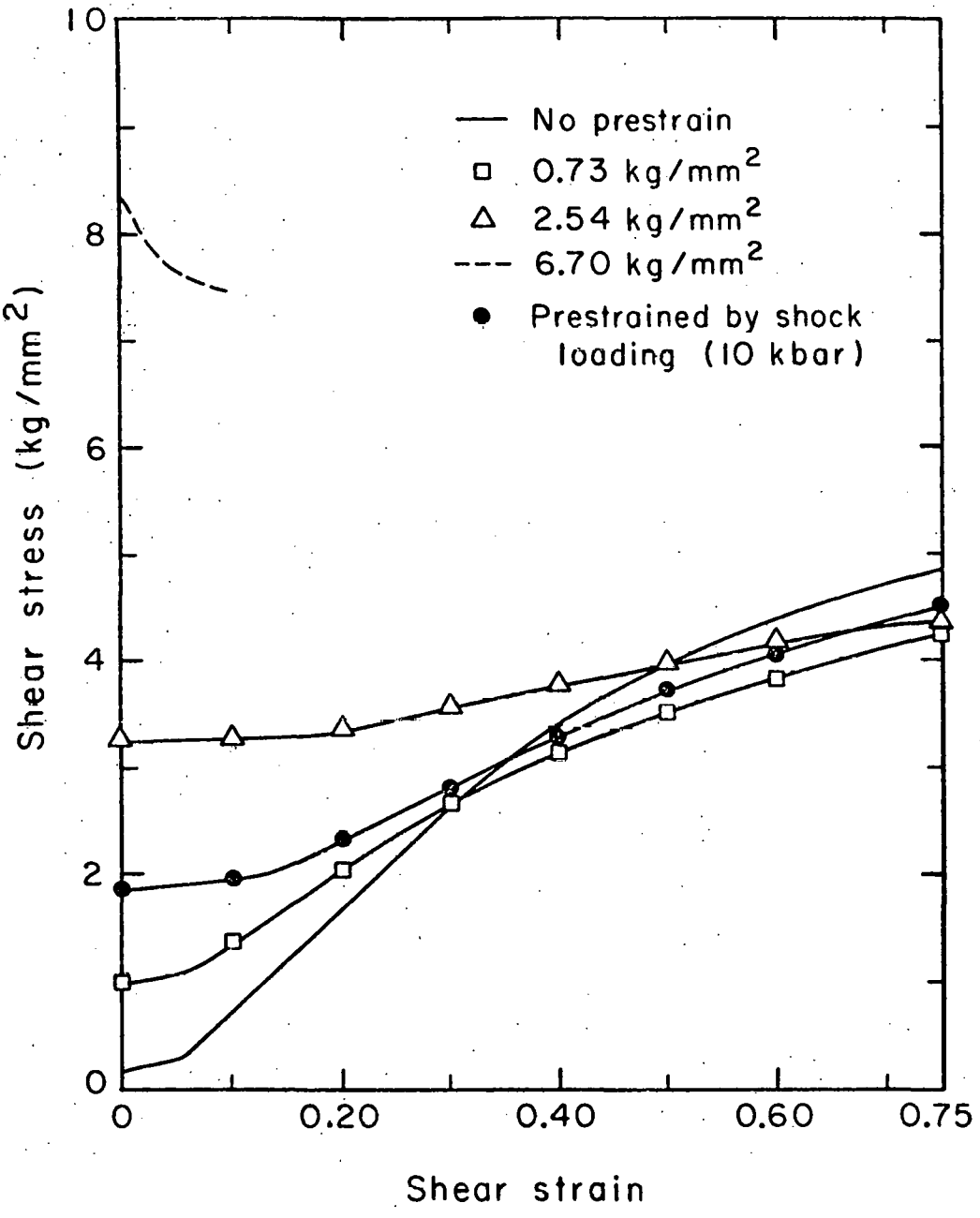
10
8
6
4
2
0
0
0.20
0.40
0.60
0.75
Shear stress (kg/mm²)
Shear strain
No prestrain
0.73 kg/mm²
2.54 kg/mm²
6.70 kg/mm²
Prestrained by shock loading (10 kbar)
MUB-11514

Fig. 1.

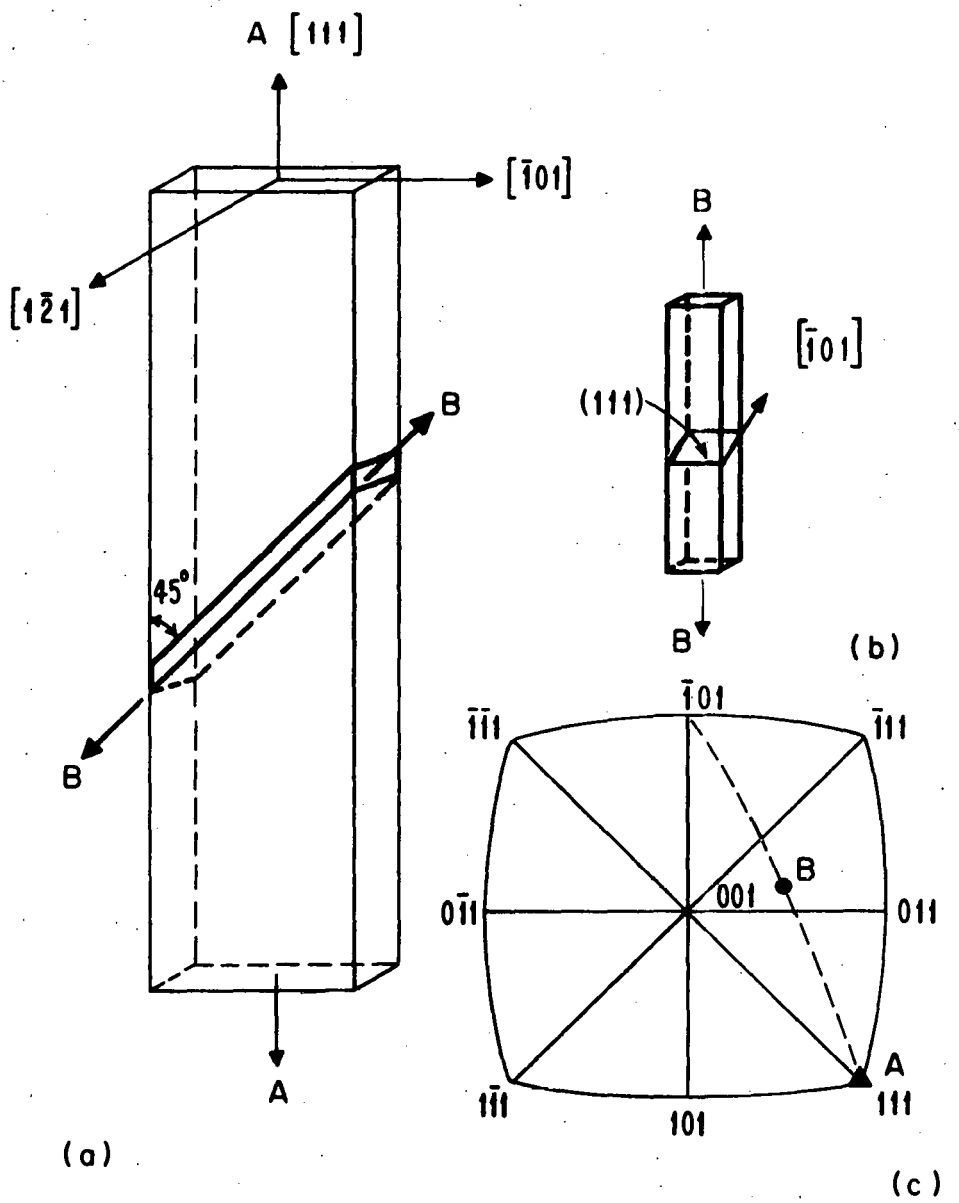

MUB 11515

Fig. 2.

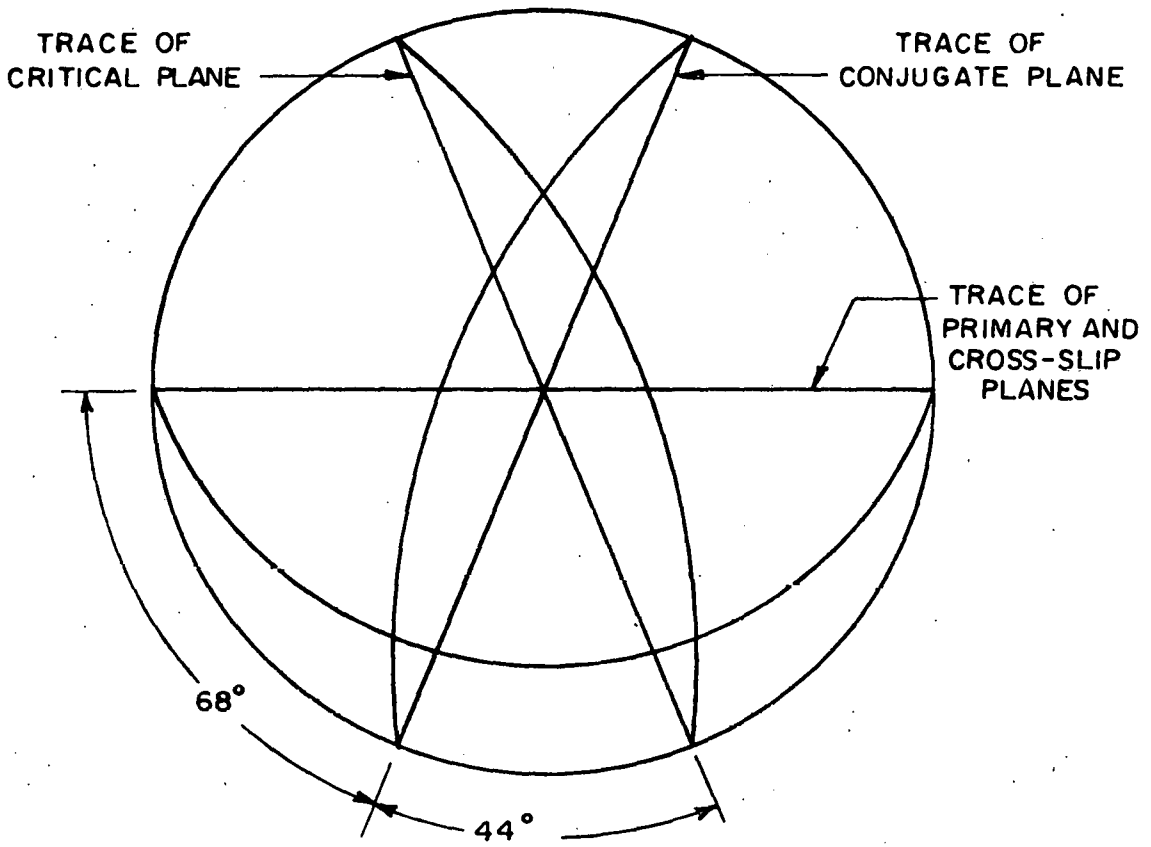
TRACE OF
CRITICAL PLANE
TRACE OF
CONJUGATE PLANE
TRACE OF
PRIMARY AND
CROSS-SLIP
PLANES
68°
44°
XBL 7012-7221

Fig. 3a

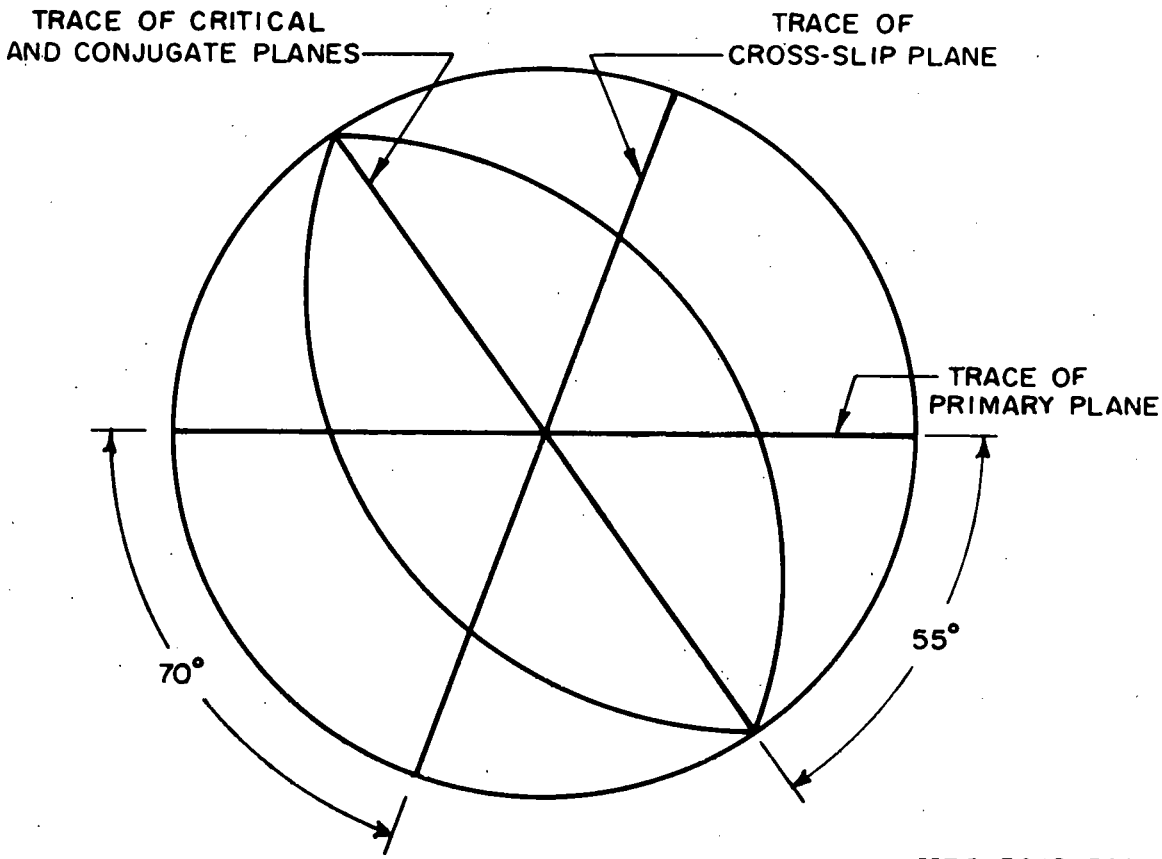
TRACE OF CRITICAL
AND CONJUGATE PLANES
TRACE OF
CROSS-SLIP PLANE
TRACE OF
PRIMARY PLANE
70°
55°
XBL 7012-7222

Fig. 3b

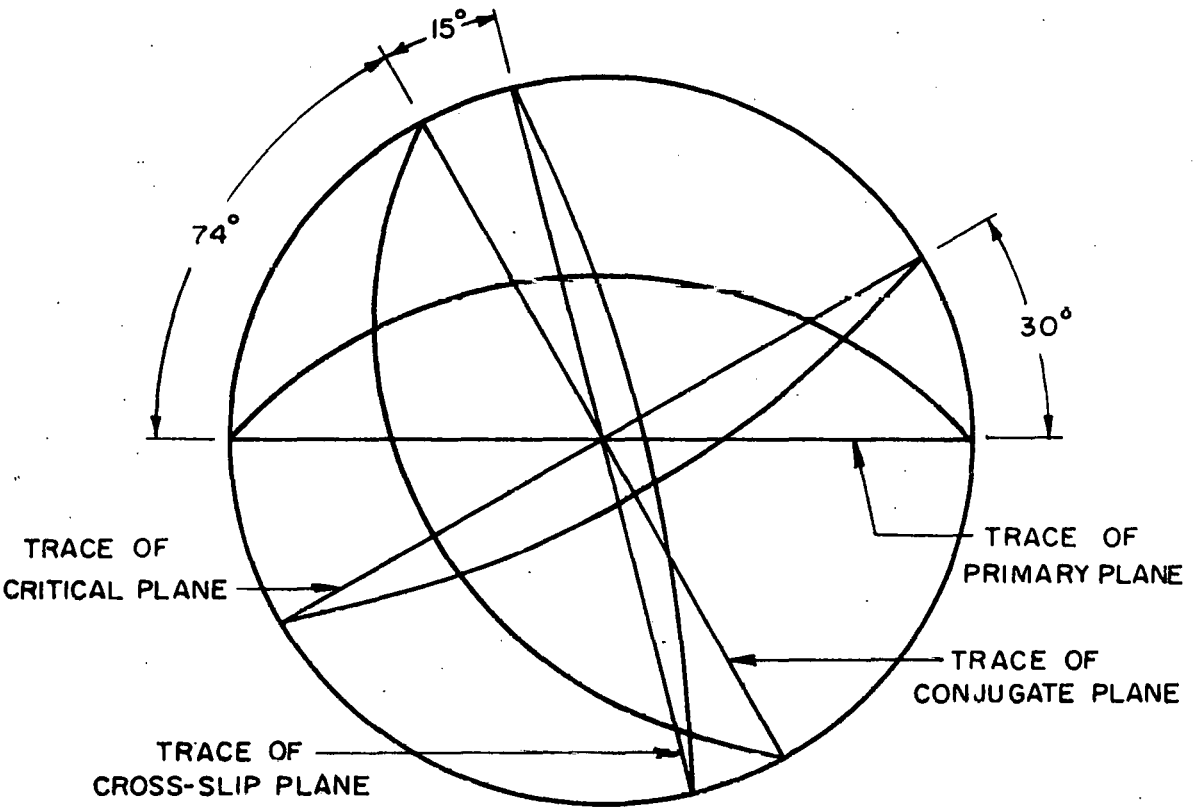

XBL 7012-7220

Fig. 3c

XBB7011-5216

Fig. 4

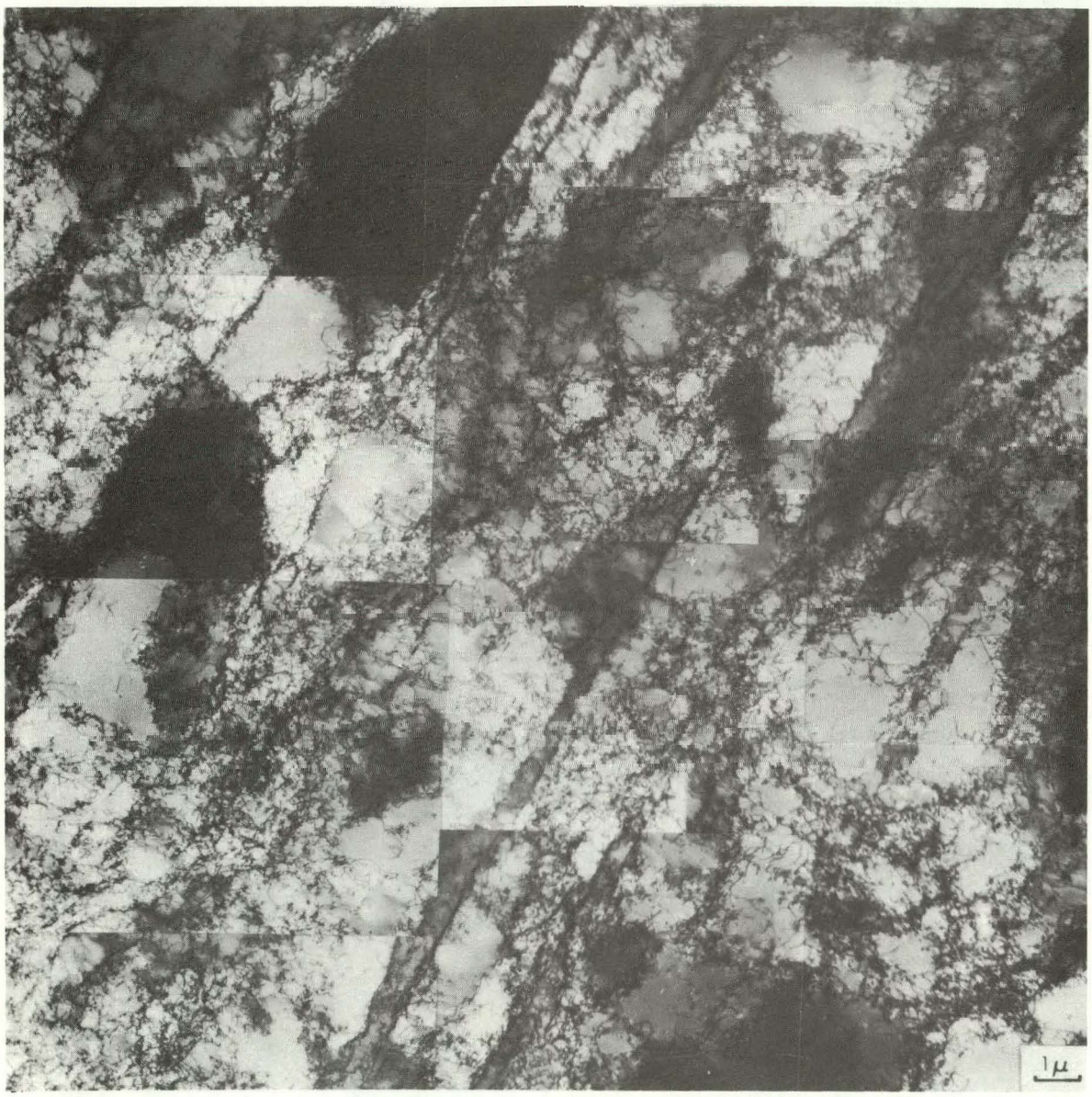

XBB7011-5219

Fig. 5

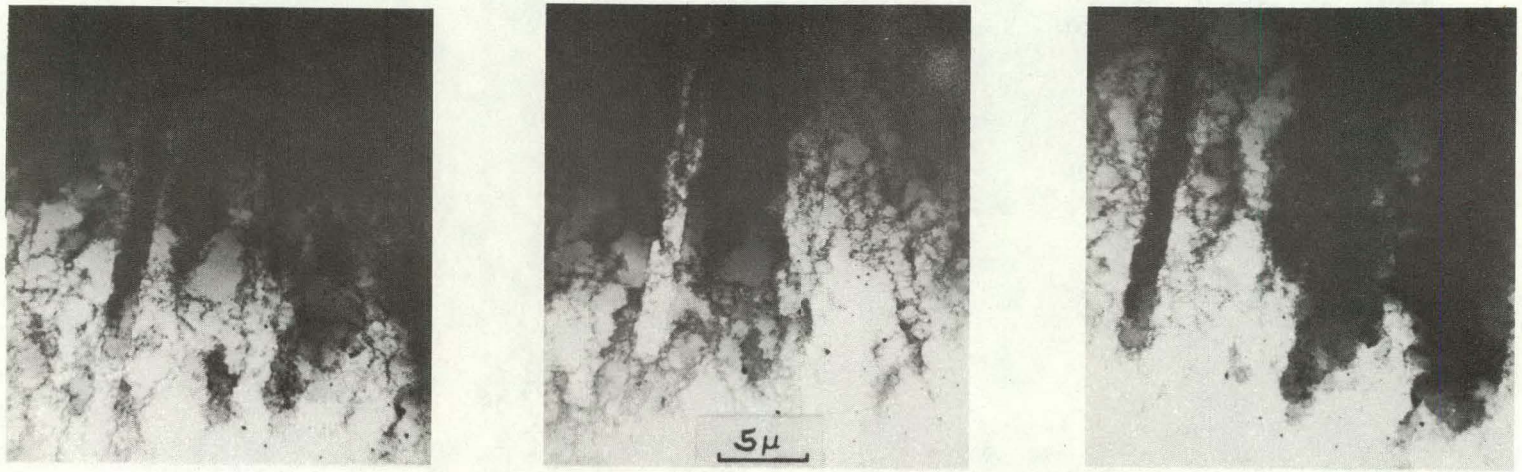

XBB708-3693

Fig. 6.

(a)

(b)

XBB7012-5352

Fig. 7.

a

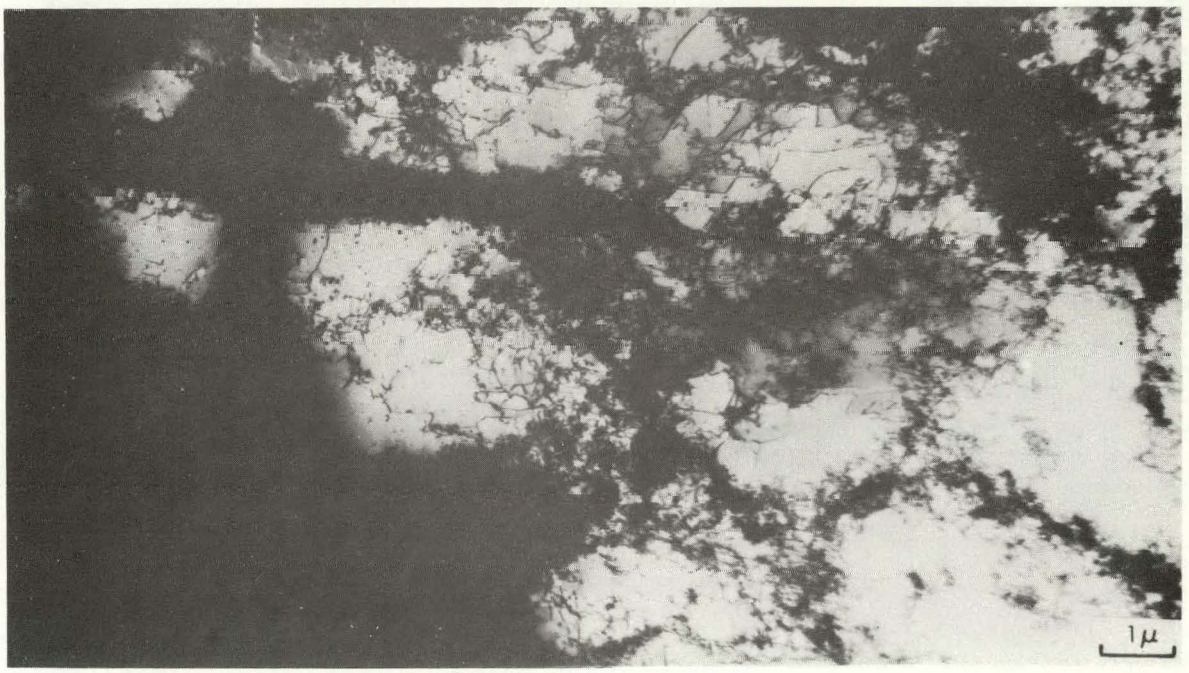

XBB7011-5214

b

Fig. 8

XBB7011-5217

Fig. 9

XBB7011-5218

Fig. 10

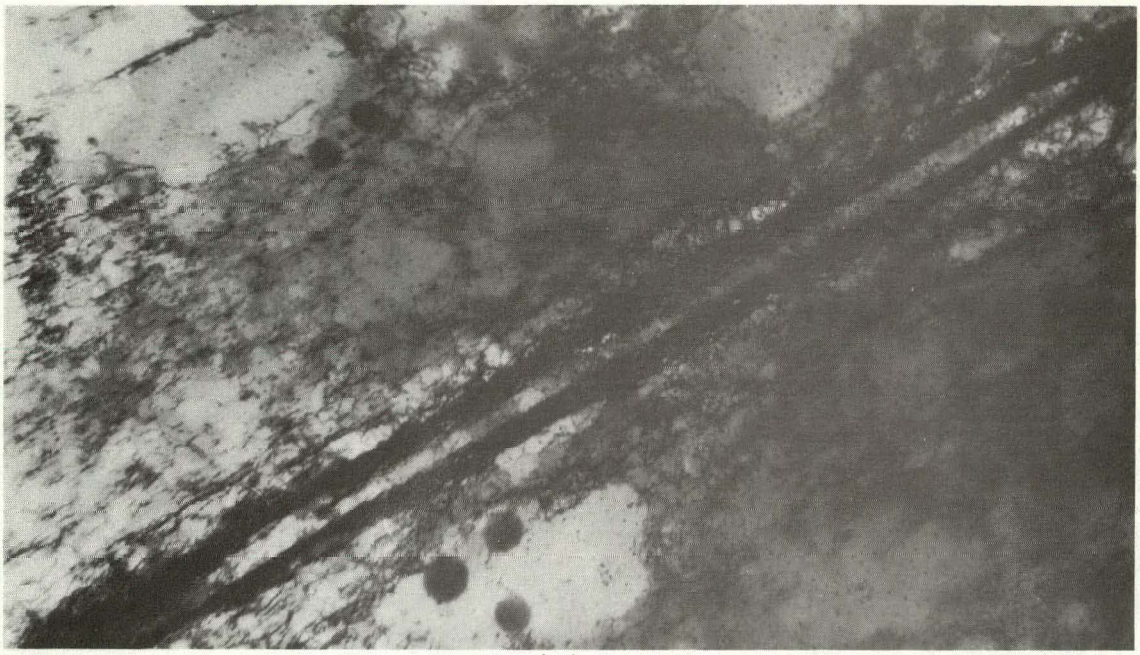

(a)

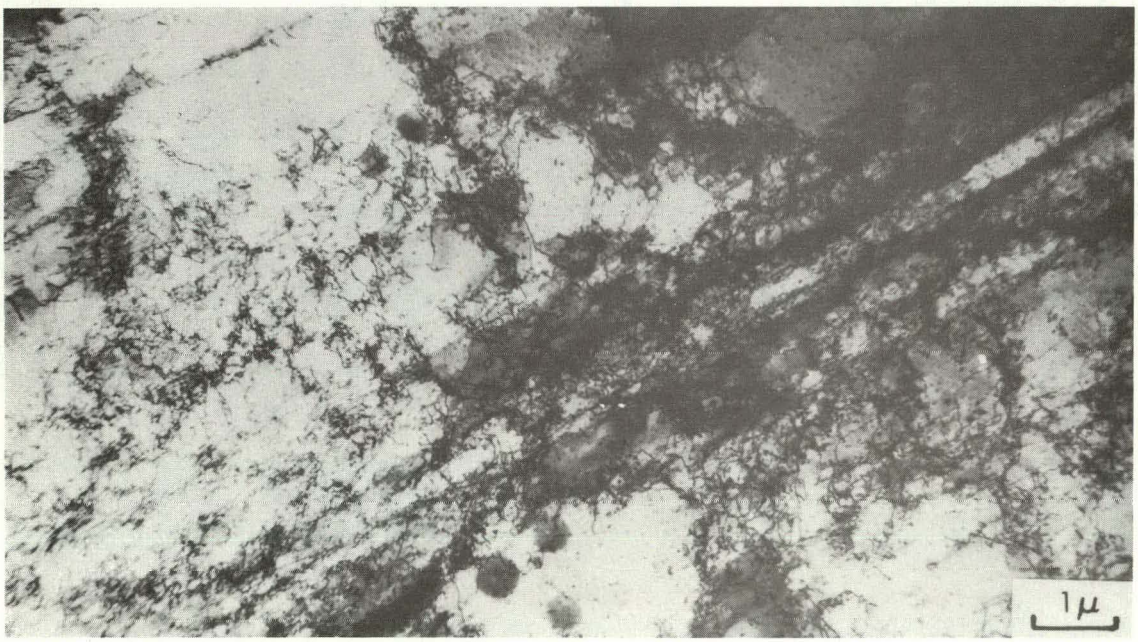

(b)

XBB 7011-5215

Fig. 11

a

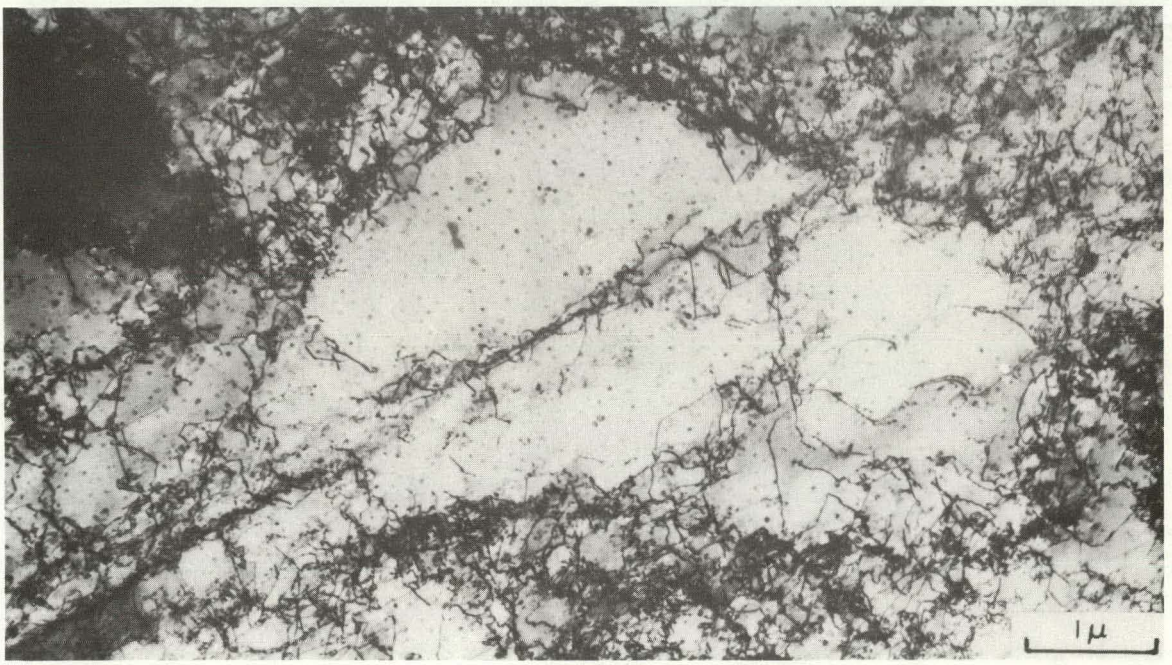

b

XBB7011-5213

Fig. 12

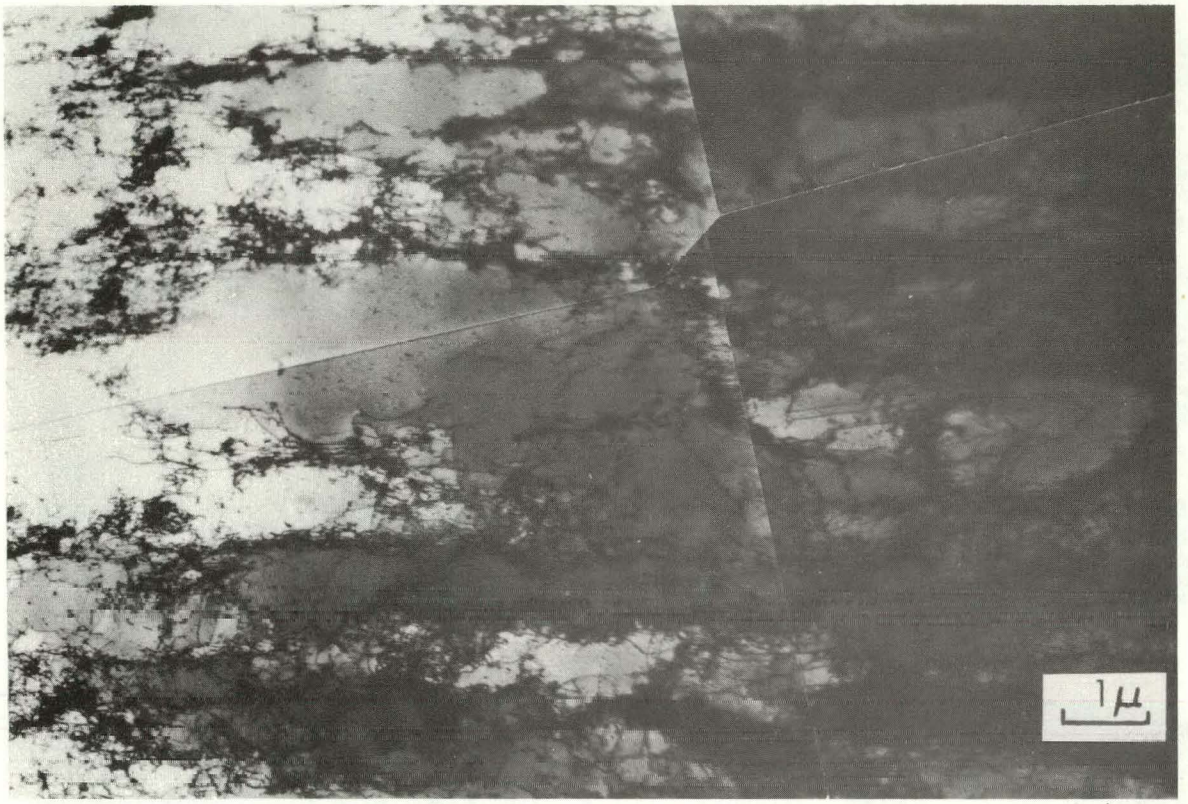

XBB7010-4512

Fig. 13

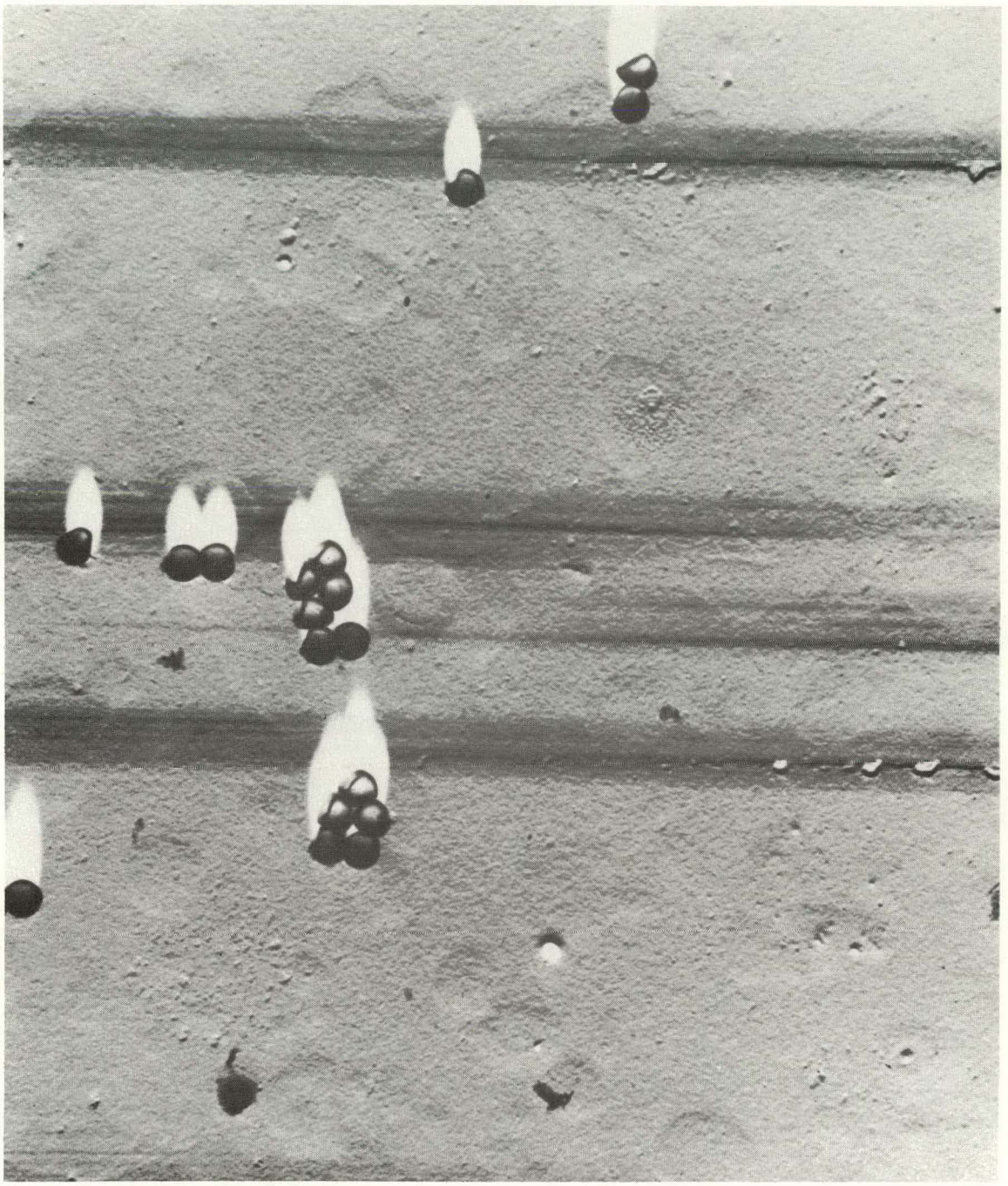

Fig. 14

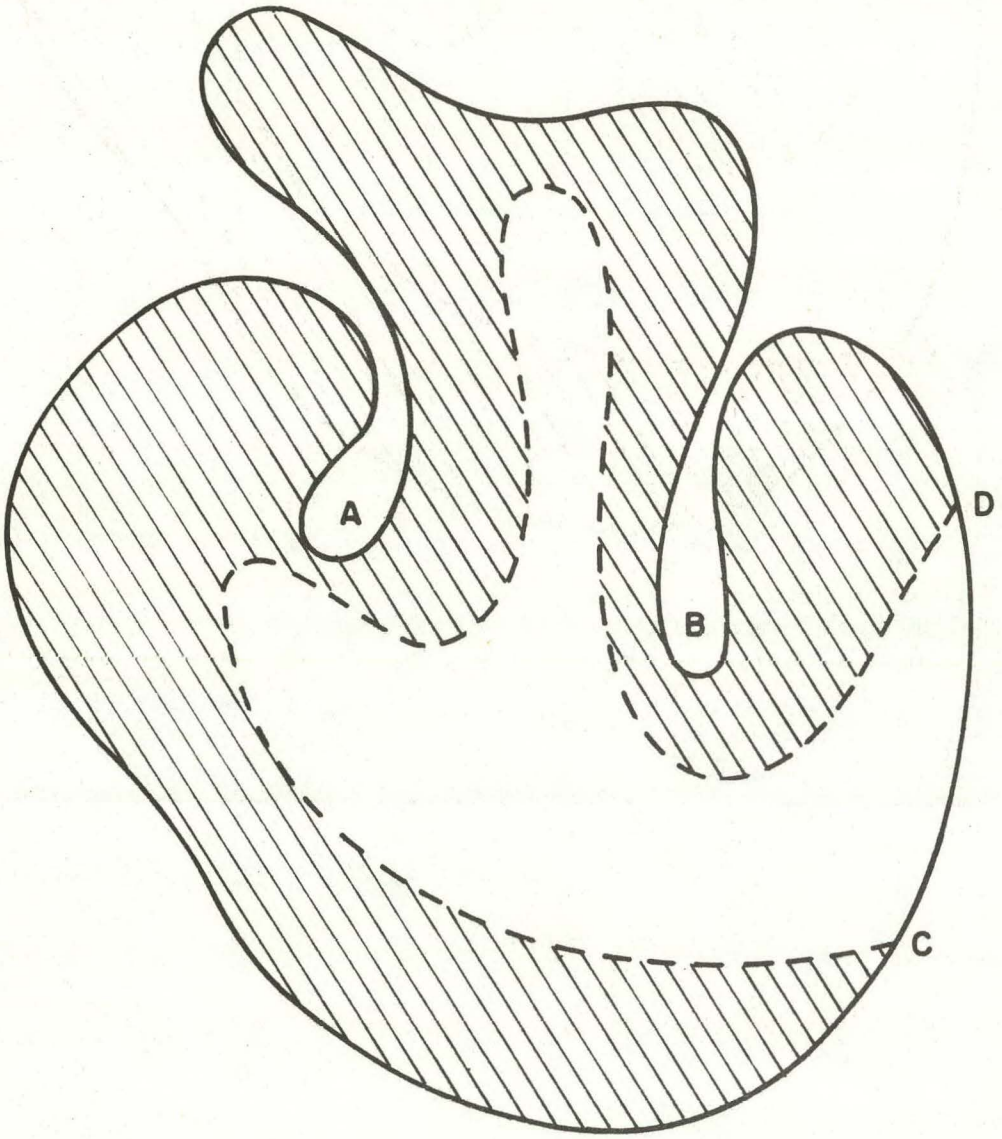

XBL 7012-7219

Fig. 15

TECHNICAL INFORMATION DIVISION
LAWRENCE RADIATION LABORATORY
UNIVERSITY OF CALIFORNIA
BERKELEY, CALIFORNIA 94720